Modeling of a fluid-structure coupled system using port-Hamiltonian formulation ⋆

Flávio Luiz Cardoso-Ribeiro * **Denis Matignon** **
Valérie Pommier-Budinger **

* *Université de Toulouse - ISAE-SUPAERO, 31055 Toulouse, France, on leave of absence from Instituto Tecnólogico of Aeronáutica, Brazil, with financial support by CNPq-Brazil, (e-mail: flaviocr@ita.br).*
** *Université de Toulouse - ISAE-SUPAERO, 31055 Toulouse, France, (e-mail: denis.matignon@isae.fr, valerie.budinger@isae.fr)*

Abstract: The interactions between fluid and structural dynamics are an important subject of study in several engineering applications. In airplanes, for example, these coupled vibrations can lead to structural fatigue, noise and even instability. At ISAE, we have an experimental device that consists of a cantilevered plate with a fluid tank near the free tip. This device is being used for model validation and active control studies. This work uses the port-Hamiltonian systems formulation for modeling this experimental device. Structural dynamics and fluid dynamics are independently modeled as infinite-dimensional systems. The plate is approximated as a beam. Shallow water equations are used for representing the fluid in the moving tank. The global system is coupled and spatial discretization of the infinite-dimensional systems using mixed finite-element method allows to obtain a finite-dimensional system that is still port-Hamiltonian.

Keywords: Port-Hamiltonian systems, fluid-structure, mixed finite-elements, active control.

1. INTRODUCTION

The coupling between structural dynamics and fluid dynamics is a major concern in several engineering applications. A popular example is the aerodynamics and structural dynamics coupling which can lead to instability and structural failure in systems as diverse as airplanes and suspension bridges.

This paper is part of ongoing research on fluid-structure modeling and control. We have an experimental set up at ISAE, which consists of an aluminium plate with a water tank near the free tip. The fluid dynamics and structural dynamics have similar natural vibration frequencies, leading to strong dynamic coupling between them. Piezoelectric patches are used for active control. A schematic representation of the system is presented in Fig. 1.

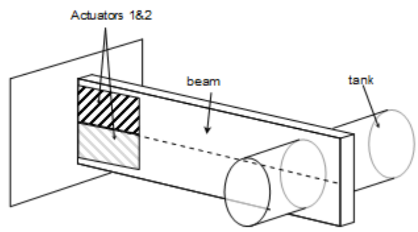

Fig. 1. Experimental set up schematic representation

In this work, port-Hamiltonian systems (PHS) formulation is used in order to model this device. The motivation for using this formulation is that it is possible to describe each element of the system separately using PHS formulation. Physically relevant variables appear as interconnection ports and the several subsystems can be coupled, guaranteeing that the global system is also a PHS. Finally, energy-based methods can be used for control purposes, see Duindam et al. (2009).

The plate is simplified as a 1D-beam with bending and torsion modeled independently. Linear Euler-Bernoulli equation is used for beam bending and wave equation for beam torsion. For the fluid dynamics, previous work on shallow water equations (as Hamroun et al. (2010)) was extended to include rigid body motion variables. In addition, (finite-dimensional) rigid body equations is used to include the dynamics of the rigid tank. Each subsystem is presented in Section 2.

The global system consists in three infinite-dimensional port-Hamiltonian subsystems and three finite-dimensional ones. Using kinematic and force/moment constraints, all subsystems are coupled in Section 3. Since no dissipation is taken into account in any of the components, the coupled system is proved to be power-conserving.

Then, the mixed finite-element method is used to perform spatial discretization of the system, as presented in Section 4. This leads to finite-dimensional port-Hamiltonian systems, with input/output ports that are directly related

⋆ This work was partially supported by ANR-project HAMECMOPSYS ANR-11-BS03-0002.

to the interconnection structure. Using the coupling constraints, the discretized system is finally written in linear descriptor form.

2. MODELING

2.1 Beam equations - bending

The simplest mathematical representation of beam vibration in bending is given by the Euler-Bernoulli equation:

$$\mu(z)\frac{\partial^2}{\partial t^2}w(z,t) = -\frac{\partial^2}{\partial z^2}\left(EI(z)\frac{\partial^2}{\partial z^2}w(z,t)\right), \qquad (1)$$

where $w(z,t)$ is the deflection at point z and time t, μ is the beam mass per unit length and E is Young modulus, I the section inertia.

Defining the energy variables as: $x_1^B(z,t) := \frac{\partial^2 w}{\partial z^2}$ and $x_2^B(z,t) := \mu\frac{\partial w}{\partial t}$, we have the following Hamiltonian:

$$H^B(x_1^B, x_2^B) = \frac{1}{2}\int_{z=0}^{L}\left(EI(x_1^B)^2 + \frac{1}{\mu}(x_2^B)^2\right)dz, \qquad (2)$$

where $\frac{1}{2}\int_{z=0}^{L}\left(EI(x_1^B)^2\right)dz$ is the elastic potential energy and $\frac{1}{2}\int_{z=0}^{L}\left(\frac{1}{\mu}(x_2^B)^2\right)dz$ is the kinetic energy.

The variational derivative of H, with respect to x_1^B and x_2^B is given by:

$$e_1^B(z,t) := \frac{\delta H^B}{\delta x_1^B} = EIx_1^B = EI\frac{\partial^2 w}{\partial z^2}, \qquad (3)$$

$$e_2^B(z,t) := \frac{\delta H^B}{\delta x_2^B} = \frac{x_2^B}{\mu} = \frac{\partial w}{\partial t}, \qquad (4)$$

where e_1^B and e_2^B are the effort (or co-energy) variables: e_1^B is the local bending moment ($EI\frac{\partial^2 w}{\partial z^2}(z,t)$) and e_2^B is the local vertical speed $\frac{\partial w}{\partial t}(z,t)$.

We can rewrite the Euler-Bernoulli beam equations using these new variables as follows:

$$\frac{\partial}{\partial t}\begin{bmatrix} x_1^B \\ x_2^B \end{bmatrix} = \begin{bmatrix} 0 & -\partial_{z^2}^2 \\ \partial_{z^2}^2 & 0 \end{bmatrix}\begin{bmatrix} e_1^B \\ e_2^B \end{bmatrix}. \qquad (5)$$

We can now compute the Hamiltonian rate of change:

$$\begin{aligned} \dot{H}^B &= \int_{z=0}^{L}\left(EIx_1^B\frac{\partial x_1^B}{\partial t} + \frac{1}{\mu}x_2^B\frac{\partial x_2^B}{\partial t}\right)dz \qquad (6)\\ &= \int_{z=0}^{L}\left(e_1^B(\frac{\partial^2 e_2^B}{\partial^2 z}) - e_2^B\frac{\partial^2 e_1^B}{\partial z^2}\right)dz \\ &= \int_{z=0}^{L}\frac{\partial}{\partial z}\left(e_1^B\frac{\partial e_2^B}{\partial z} - e_2^B\frac{\partial e_1^B}{\partial z}\right)dz \\ &= e_1^B(L,t)\frac{\partial}{\partial z}e_2^B(L,t) - \frac{\partial}{\partial z}e_1^B(L,t)e_2^B(L,t) + \\ &\quad - e_1^B(0,t)\frac{\partial}{\partial z}e_2^B(0,t) + \frac{\partial}{\partial z}e_1^B(0,t)e_2^B(0,t). \end{aligned}$$

Notice that the energy exchange depends only on the system's boundary conditions; we define: $e_{1\partial}^B := \frac{\partial}{\partial z}e_1^B = \frac{\partial}{\partial z}EI\frac{\partial^2 w}{\partial z^2}$, the shear force, and $e_{2\partial}^B := \frac{\partial}{\partial z}e_2^B = \frac{\partial}{\partial t}\frac{\partial w}{\partial z}$, the angular velocity.

In the clamped-free beam, for example, the following boundary conditions apply:

- Clamped end: $e_2^B(0,t) = 0$ and $e_{2\partial}^B(0,t) = 0$;
- Free end: $e_1^B(L,t) = 0$ and $e_{1\partial}^B(L,t) = 0$.

In this specific case, the system is power-conserving: $\dot{H}^B = 0$. In our case, the flexible beam is connected to a rigid tank with fluid, so that the free-end boundary conditions will not be zero.

Instead of using a free-end boundary, we can specify as boundary conditions the values of force and bending moment applied by the connected structure. The value of force/moment ($f(t)$ and $m^B(t)$) are given by:

$$e_1^B(L,t) = m^B(t) \qquad (7)$$

$$e_{1\partial}^B(L,t) = f(t) \qquad (8)$$

The conjugate port-variables are given by the point speed and angular velocity, respectively.

2.2 Beam equations - torsion

The equations of a beam in torsion can be approximated by [1]:

$$\frac{\partial}{\partial z}\left(GJ\frac{\partial}{\partial z}\theta(z,t)\right) = I_p\frac{\partial^2}{\partial t^2}\theta(z,t), \quad 0 \le z \le L, \qquad (9)$$

where $\theta(z,t)$ is the local torsional angle, z is the position along the beam, t is time, G is the material shear constant, J is the section torsion constant and I_p is the section polar moment of inertia per unit length. Defining as energy variables $x_1^T := \frac{\partial\theta}{\partial z}$ and $x_2^T := I\frac{\partial\theta}{\partial t}$, we have:

$$\frac{\partial}{\partial t}\begin{bmatrix} x_1^T \\ x_2^T \end{bmatrix} = \begin{bmatrix} 0 & \partial_z \\ \partial_z & 0 \end{bmatrix}\begin{bmatrix} e_1^T \\ e_2^T \end{bmatrix}. \qquad (10)$$

Where $e_1^T = GJx_1^T = GJ\frac{\partial w}{\partial z}$ and $e_2^T = \frac{x_1^T}{I} = \frac{\partial\theta}{\partial t}$, which are the variational derivatives of the Hamiltonian, given by:

$$H^T(x_1^T, x_2^T) = \frac{1}{2}\int_{z=0}^{L}\left(GJ(x_1^T)^2 + \frac{(x_2^T)^2}{I_p}\right)dz. \qquad (11)$$

Notice that e_1^T is the moment of torsion and e_2^T is the torsion angular velocity. The time-derivative of the Hamiltonian can be computed as:

$$\dot{H}^T(x_1^T, x_2^T) = e_1^T(L,t)e_2^T(L,t) - e_1^T(0,t)e_2^T(0,t). \qquad (12)$$

Again, it is possible to see that the energy flows through the boundaries. In the fixed-free case, for example, the following boundary conditions apply:

- Fixed end: $e_2^T(0,t) = 0$;
- Free end: $e_1^T(L,t) = 0$.

And the system is power conserving: $\dot{H}^T = 0$.

Instead of using a free-end boundary, we can specify as boundary conditions at $z = L$ the value of the torsion moment applied by the connected structure. The value of moment ($\tau(t)$) would be an input of the system:

$$e_1^T(L,t) = \tau(t) \qquad (13)$$

The conjugate port-variable is given by the angular velocity at the same point.

[1] This equation considers Saint-Venant theory of torsion. In addition, it is considered that torsion is uncoupled from transverse deflection. A detailed derivation of this equation is presented by Hodges and Pierce (2011) (section 2.3.1)

2.3 Rigid tank

Let us consider a rigid tank with three degrees of freedom, two related to the bending motion of the beam (translation $w_B(t)$ and rotation $\theta_B(t)$), and one rotation degree of freedom related to torsion ($\theta_T(t)$).

The equations of motion are given directly by Newton's second law:

$$m_{RB}\,\ddot{w}_B(t) = F_{\text{ext}}, \tag{14}$$

$$I_{RB}^B\,\ddot{\theta}_B(t) = M_{\text{ext,B}}, \tag{15}$$

$$I_{RB}^T\,\ddot{\theta}_T(t) = M_{\text{ext,T}}, \tag{16}$$

where m_{RB} is the tank mass, I_{RB}^B and I_{RB}^T are the tank rotational inertias. F_{ext} is the sum of forces applied to the tank, $M_{\text{ext,B}}$ is the sum of moments in bending direction and $M_{\text{ext,T}}$ is the sum of moments in torsion direction.

Defining the following moment variables: $p := m_{RB}\dot{w}_B$, $p_{\theta B} := I_{RB}^B\dot{\theta}_B$, and $p_{\theta T} := I_{RB}^T\dot{\theta}_T$, we can rewrite the previous equations as:

$$\frac{\partial}{\partial t}\begin{bmatrix} p \\ w_B \end{bmatrix} = \begin{bmatrix} 0 & -1 \\ 1 & 0 \end{bmatrix}\begin{bmatrix} \partial_p H^{RB} \\ \partial_{w_b} H^{RB} \end{bmatrix} + \begin{bmatrix} 1 \\ 0 \end{bmatrix} F_{\text{ext}}, \tag{17}$$

$$\frac{\partial}{\partial t}\begin{bmatrix} p_{\theta B} \\ \theta_B \end{bmatrix} = \begin{bmatrix} 0 & -1 \\ 1 & 0 \end{bmatrix}\begin{bmatrix} \partial_{p_{\theta M}} H^{RB} \\ \partial_{\theta_B} H^{RB} \end{bmatrix} + \begin{bmatrix} 1 \\ 0 \end{bmatrix} M_{\text{ext,B}}, \tag{18}$$

$$\frac{\partial}{\partial t}\begin{bmatrix} p_{\theta T} \\ \theta_T \end{bmatrix} = \begin{bmatrix} 0 & -1 \\ 1 & 0 \end{bmatrix}\begin{bmatrix} \partial_{p_{\theta T}} H^{RB} \\ \partial_{\theta_T} H^{RB} \end{bmatrix} + \begin{bmatrix} 1 \\ 0 \end{bmatrix} M_{\text{ext,T}}, \tag{19}$$

where the Hamiltonian is equal to the kinetic energy:

$$H^{RB}(p, p_{\theta B}, p_{\theta T}) = \frac{1}{2}\left(\frac{p^2}{m_{RB}} + \frac{p_{\theta B}^2}{I_{RB}^B} + \frac{p_{\theta T}^2}{I_{RB}^T}\right), \tag{20}$$

and its rate of change is given by:

$$\begin{aligned} \dot{H}^{RB} &= \dot{w}_B\dot{p} + \dot{\theta}_B\dot{p}_{\theta B} + \dot{\theta}_T\dot{p}_{\theta T} \\ &= \dot{w}_B F_{\text{ext}} + \dot{\theta}_B M_{\text{ext,B}} + \dot{\theta}_T M_{\text{ext,T}}\,. \end{aligned} \tag{21}$$

2.4 Sloshing fluid

The simplest infinite-dimensional approach for modeling the sloshing fluid dynamics is the Saint-Venant equations in 1D. These equations are obtained under the following hypotheses: non viscous, incompressible fluid and little depth of fluid in comparison to the tank length (for this reason, these equations are also known as *shallow water* equations). A derivation of Saint-Venant equations for tanks under rigid-body motion is presented by Petit and Rouchon (2002). We rewrite here the linear version as:

$$\frac{\partial\tilde{h}}{\partial t} = -\frac{\partial}{\partial z}(\bar{h}v) \tag{22}$$

$$\frac{\partial v}{\partial t} = -\frac{\partial}{\partial z}\left(g\tilde{h} + gz\theta_F\right) \tag{23}$$

where $v(z,t)$ is the fluid speed at point z and time t, $\tilde{h}(z,t)$ is the fluid height relative to static (equilibrium) height $\bar{h}$ (the total height is thus $h(z,t) = \bar{h} + \tilde{h}(z,t)$), g is the gravity acceleration and $\theta_F(t)$ is the tank rotation angle.

The fluid kinetic energy is given by:

$$T(\tilde{h}, \theta_F, \dot{\theta}_F) = \frac{\rho b}{2}\int_{-a/2}^{a/2} \bar{h}\left(v^2 + (z\dot{\theta}_F)^2\right)dz, \tag{24}$$

where ρ is the fluid density, b is the tank width, a is the tank length and $\dot{\theta}_F(t)$ is the tank rotation velocity.

The fluid gravitational potential energy is given by:

$$U(\tilde{h}, \theta_F, \dot{\theta}_F) = \rho bg\int_{-a/2}^{a/2}\left(z\tilde{h}\theta_F + \frac{\tilde{h}^2}{2}\right)dz, \tag{25}$$

the Hamiltonian is given by $H^F = U + T$. Defining $\alpha_1 := \frac{\tilde{h}}{\bar{h}}$, the relative height, and $\alpha_2 := \rho\bar{h}bv$, the mass flow rate:

$$\begin{aligned} H^F = &\int_{-a/2}^{a/2}\left(\rho bg\bar{h}^2\frac{\alpha_1^2}{2} + \frac{\alpha_2^2}{2\rho\bar{h}b} + \rho bgx\bar{h}\alpha_1\theta\right)dz \\ &+ \underbrace{\left(\int_{-a/2}^{a/2}\rho b\bar{h}z^2 dz\right)}_{I_f}\frac{\dot{\theta}_F^2}{2} \end{aligned} \tag{26}$$

Notice that I_f is a constant (the equivalent "rigid" inertia of the fluid).

Defining the fluid rotation momentum as $p_F(t) := I_f\dot{\theta}(t)$, we rewrite the Hamiltonian as a function of these variables:

$$\begin{aligned} H^F := &\int_{-a/2}^{a/2}\left(\rho bg\bar{h}^2\frac{\alpha_1^2}{2} + \frac{\alpha_2^2}{2\rho\bar{h}b} + \rho bgx\bar{h}\alpha_1\theta\right)dz \\ &+ \frac{p_F^2}{2I_f} \end{aligned} \tag{27}$$

The co-energy variables are given by the variational derivative of H^F with respect to the infinite-dimensional energy variables $\alpha_1(z,t)$ and $\alpha_2(z,t)$, and the partial derivative with respect to the finite-dimensional variables $\theta_F(t)$ and $p_F(t)$:

$$e_1^F(z,t) := \frac{\delta}{\delta\alpha_1}H^f = \rho bg\bar{h}^2\alpha_1 + \rho bg\bar{h}z\theta_F \tag{28}$$

$$e_2^F(z,t) := \frac{\delta}{\delta\alpha_2}H^f = \frac{\alpha_2}{\rho\bar{h}b} = v \tag{29}$$

$$e_\theta^F(t) := \frac{\partial}{\partial\theta_F}H^f = \rho bg\int_{-a/2}^{a/2} hzdz \tag{30}$$

$$e_p^F(t) := \frac{\partial}{\partial p_F}H^f = \frac{p}{I_f} = \dot{\theta}_F \tag{31}$$

Notice that $e_1^F(z,t)$ is the local pressure relative to equilibrium, multiplied by the fluid section area ($b\bar{h}$), $e_2^F(z,t)$ is the local fluid speed. In addition: e_θ^F is the torque due to fluid pressure and e_p^F is the rotation velocity of the tank.

We can rewrite Saint-Venant equations using these new variables:

$$\frac{\partial}{\partial t}\begin{bmatrix} \alpha_1 \\ \alpha_2 \end{bmatrix} = \begin{bmatrix} 0 & -\partial_z \\ -\partial_z & 0 \end{bmatrix}\begin{bmatrix} e_1^F \\ e_2^F \end{bmatrix}. \tag{32}$$

In addition, we can find the equations of motion that describe the rotation of the tank:

$$\frac{\partial}{\partial t}p_F(t) = -e_\theta^F + M_{\text{ext}}, \tag{33}$$

$$\frac{\partial}{\partial t}\theta_F(t) = e_p^F. \tag{34}$$

In matrix form, we get:

$$\frac{\partial}{\partial t}\begin{bmatrix} \alpha_1 \\ \alpha_2 \\ p_F \\ \theta_F \end{bmatrix} = \begin{bmatrix} 0 & -\partial_z & 0 & 0 \\ -\partial_z & 0 & 0 & 0 \\ 0 & 0 & 0 & -1 \\ 0 & 0 & 1 & 0 \end{bmatrix}\begin{bmatrix} e_1^F \\ e_2^F \\ e_p^F \\ e_\theta^F \end{bmatrix} + \begin{bmatrix} 0 \\ 0 \\ 1 \\ 0 \end{bmatrix} M_{\text{ext}}^F \tag{35}$$

The time-derivative of H^F can be computed as:

$$\dot{H}^F = e_1^F(-a/2,t)e_2^F(-a/2,t) - e_1^F(a/2,t)e_2^F(a/2,t) + \dot{\theta}M \tag{36}$$

Notice that the rate of change of the Hamiltonian is a function of the boundary conditions (speed and force applied to the tank walls) and moment/ rotation velocity of the tank.

3. COUPLING

It is now time to couple all the elements of the system. First, we notice that several kinematic constraints appear, due to the coupling at the interconnection point:

- Translation speeds of each subsystem are equal (3 constraints):
$$\dot{w}_B = e_2^B(L,t) = e_2^F(-a/2,t) = e_2^F(a/2,t) \tag{37}$$
- Rotation speeds in bending are equal (1 constraint):
$$\dot{\theta}_B = \frac{\partial e_2^B}{\partial z}(L,t) \tag{38}$$
- Rotation speeds in torsion are equal (2 constraints):
$$\dot{\theta}_T = e_2^T(L,t) = \dot{\theta}_F \tag{39}$$

The Hamiltonian of the global system is given by the sum of each Hamiltonian component (Eqs. 2, 11, 20 and 27):

$$H = H^B + H^T + H^{RB} + H^F. \tag{40}$$

Then, by using the sum of each Hamiltonian component rate of change (Eqs. 6, 12, 21 and 36), and imposing the previous kinematic constraints, we obtain the following global Hamiltonian rate of change:

$$\begin{aligned}\dot{H} = &+ \dot{w}_B \underbrace{\left(-\frac{\partial}{\partial z}e_1^B(L,t) + F_{\text{ext}} - e_1^F(a/2,t) + e_1^F(-a/2,t)\right)}_{F_\Sigma} \\ &+ \dot{\theta}_B \underbrace{\left(e_1^B(L,t) + M_{\text{ext,B}}\right)}_{M_{\Sigma,B}} \\ &+ \dot{\theta}_T \underbrace{\left(e_1^T(L,t) + M_{\text{ext,T}} + M_{\text{ext}}\right)}_{M_{\Sigma,T}}.\end{aligned} \tag{41}$$

Notice that F_Σ, $M_{\Sigma,B}$ and $M_{\Sigma,T}$ are the sum of external forces/moments applied to each subsystem. From a global system perspective, they are the sum of internal forces/moments at the interconnection point, which should be equal to zero:

$$F_\Sigma = 0, \tag{42}$$
$$M_{\Sigma,B} = 0, \tag{43}$$
$$M_{\Sigma,T} = 0. \tag{44}$$

Since no damping has been taken into account in the modeling of the different components, the global system is power conserving (notice however that exchanges of energy between subsystems are allowed). Hence, $\dot{H}$ should be equal to zero, which is the case when imposing these constraints.

Remark. From a control perspective, it could be an interesting idea to propose feedback laws such as an external actuator applying forces and moments at the coupling point: $F_\Sigma = -k_1\dot{w}_B$, $M_{\Sigma,B} = -k_2\dot{\theta}_B$ and $M_{\Sigma,T} = -k_3\dot{\theta}_T$, with $k_1, k_2, k_3 \geq 0$. This would guarantee that $\dot{H} \leq 0$ and stabilization would be achieved. When $k_i = 0$ (no feedback), we recover the power-conserving case above.

4. SPATIAL DISCRETIZATION

Equations for the beam and fluid dynamics are given by partial differential equations (PDEs) written in the following form (Eqs. 5, 10 and 32):

$$\dot{X}(z,t) = \mathcal{J}\frac{\delta H}{\delta X}, \tag{45}$$

where $\mathcal{J}$ is a formally skew-symmetric differential operator, $X(z,t)$ is a vector with two components. In the case of torsion (Eq. 10) and Saint-Venant equations (Eq. 32) $\mathcal{J}$ is a first-order operator. In the case of Euler-Bernoulli equation (Eq. 5), it is a second-order one.

The spatial discretization can be done using the mixed finite-element method, proposed by Golo et al. (2004), which leads to finite-dimensional systems of the following form:

$$\dot{\boldsymbol{x}}^i(t) = \boldsymbol{J_d^i}\frac{\partial H_d^i}{\partial \boldsymbol{x^i}} + \boldsymbol{B^i u^i}, \tag{46}$$
$$\boldsymbol{y^i} = (\boldsymbol{B^i})^T\frac{\partial H_d^i}{\partial \boldsymbol{x^i}} + \boldsymbol{D^i u^i}, \tag{47}$$

where i stands for B, T and F (bending, torsion and fluid equations), $\boldsymbol{x^i}(t)$ is a $2N^i$-dimensional vector (N^i is the number of elements), $\boldsymbol{J_d^i}$ is a $2N^i \times 2N^i$ skew-symmetric matrix, $\boldsymbol{B^i}$ is a $2N^i \times m^i$ matrix, $\boldsymbol{D^i}$ is a $m^i \times m^i$ skew-symmetric matrix, $\boldsymbol{u^i}$ and $\boldsymbol{y^i}$ are m^i-dimensional vectors with boundary co-energy variables as components. The previous matrices, as well as the discretized Hamiltonian H_d^i for each subsystem are presented in Appendix A.

Now each of the previous infinite-dimensional equations is approximated as a finite-dimensional system. In addition, rigid body equations were presented (from Eqs. 14, 15 and 16). By concatenating each state-variable as: $\boldsymbol{x} = \begin{bmatrix}\boldsymbol{x^B} & \boldsymbol{x^T} & \boldsymbol{x^{RB}} & \boldsymbol{x^F}\end{bmatrix}^T$, it is possible to rewrite the full model using exactly the same framework as for each component:

$$\dot{\boldsymbol{x}}(t) = \boldsymbol{J_d}\frac{\partial H_d}{\partial \boldsymbol{x}} + \boldsymbol{Bu}, \tag{48}$$
$$\boldsymbol{y^i} = (\boldsymbol{B})^T\frac{\partial H_d}{\partial \boldsymbol{x}} + \boldsymbol{Du}, \tag{49}$$

where $\boldsymbol{J_d}$, $\boldsymbol{B}$ and $\boldsymbol{D}$ are the block-diagonal matrices obtained from each component $\boldsymbol{J_d^i}$, $\boldsymbol{B^i}$ and $\boldsymbol{D^i}$ matrices. The discrete global Hamiltonian H_d is the sum of each H_d^i. The input and output vectors are given by:

$$\boldsymbol{u} = \begin{bmatrix} e_1^B(L) \\ e_{1\partial}^B(L) \\ e_2^T(L) \\ F_{ext}^{RB} \\ M_{ext,B}^{RB} \\ M_{ext,T}^{RB} \\ e_1^F(-a/2) \\ e_2^F(a/2) \end{bmatrix}, \quad \boldsymbol{y} = \begin{bmatrix} e_{2\partial}^B(L) \\ e_1^B(L) \\ e_1^T(L) \\ \dot{w}_B^{RB} \\ \dot{\theta}_B^{RB} \\ \dot{\theta}_T^{RB} \\ e_2^F(-a/2) \\ e_1^F(a/2) \end{bmatrix}. \tag{50}$$

The coupling between all the equations is given by the 9 kinematic and force/moment constraints (Eqs. 37, 38, 39, 42, 43 and 44). Notice that all the constraints are linear functions of these input/output variables. So we can write the constraints as:

$$\mathcal{M}y + \mathcal{N}u = 0, \tag{51}$$

where $\mathcal{M}$ and $\mathcal{N}$ are 9×9 matrices. By inspection of the discretized Hamiltonian gradients (see Appendix A), it is possible to see that they are linear functions of the system state variables:

$$\frac{\partial H_d}{\partial \boldsymbol{x}} = \boldsymbol{Q}\boldsymbol{x}. \tag{52}$$

All the previous equations can be coupled using a descriptor state-space formulation:

$$\underbrace{\begin{bmatrix} I & 0 \\ 0 & 0 \end{bmatrix}}_{E} \frac{\partial}{\partial t} \begin{bmatrix} \boldsymbol{x} \\ \boldsymbol{u} \end{bmatrix} = \underbrace{\begin{bmatrix} \boldsymbol{J_d Q} & \boldsymbol{B} \\ \mathcal{M}\boldsymbol{B}^T\boldsymbol{Q} & \mathcal{M}\boldsymbol{D} + \mathcal{N} \end{bmatrix}}_{A} \begin{bmatrix} \boldsymbol{x} \\ \boldsymbol{u} \end{bmatrix} \tag{53}$$

From the generalized eigenvalues of (E,A), it is possible to find the modes of the coupled system and to compare them to experimentally measured natural frequencies. In addition, the coupled system can be simulated using differential-algebraic numerical integration methods (see e.g. Kunkel and Mehrmann (2006), chapter 8).

5. CONCLUSIONS AND FURTHER WORK

In this paper, we presented the modeling of a fluid-structure system using port-Hamiltonian formulation. The methodology is convenient since it allows to model each component independently. Physically relevant interconnection ports naturally appear when using this formulation, and the resulting system is also port-Hamiltonian. Numerical results obtained using the methodology proposed here will be presented at the conference and can be obtained in our website [2] .

Our goal is to use energy-based methods (as Hamroun et al. (2010)) to design control laws for the coupled system, thus trying to improve the damping characteristics.

In addition to the control design, several improvements still need to be done in the modeling. First, only linear models were used in this paper. We are working on using nonlinear Saint-Venant equations to represent the fluid dynamics. In contrast to equations presented in this paper, the biggest difference is that the fluid Hamiltonian gradient will have several nonlinear terms. After spatial discretization, the resulting system will be a set of nonlinear Differential-Algebraic Equations. As we have shown in Cardoso-Ribeiro et al. (2014), experimental results exhibits nonlinear behaviour when exciting the system near resonant frequencies at high amplitudes. We expect to be able to use simulation of these nonlinear equations to reproduce the experimental results, at least qualitatively.

Further work is also needed to include piezoelectric patches (as done by Voss and Scherpen (2014)). In addition, here we considered that no dissipation occurs, which is not the case in practice and a damping model should be included (as done by Matignon and Hélie (2013)).

After including the constraints of Eq. 51 to the system presented in Eq. 48, we obtained an implicit port-Hamiltonian system. While we can use descriptor state-space models and differential-algebraic equations to simulate this system, another choice is to try a coordinate change that eliminates the constraints and makes the system explicit (as van der Schaft and Maschke (1994), Wu et al. (2014)).

The spatial discretization presented here can also be improved by using more accurate methods as the method proposed by Moulla et al. (2012) (which uses a polynomial basis, leading to higher accuracy).

An additional issue that needs to be addressed is that the use of shallow water equations is usually appropriate for modeling wave propagation in canals and oceans. Since these equations consider the hypothesis that fluid depth is much smaller than the tank length, its use is very limited for representing sloshing in tanks. A better modeling approach is needed. Incompressible Euler equations with free-surface boundary conditions are usually the way to go. However, writing these equations as a PHS is still an open challenge, at the best of the authors knowledge.

[2] http://github.com/flavioluiz/port-hamiltonian

ACKNOWLEDGEMENTS

The authors gratefully acknowledge Prof. B. Maschke and his group for welcoming Flávio Cardoso-Ribeiro in LAGEP for fruitful discussions. Section 2.4 strongly benefits from these interactions.

REFERENCES

Bassi, L., Macchelli, A., and Melchiorri, C. (2007). An Algorithm to Discretize One-Dimensional Distributed Port Hamiltonian Systems. In *Lagrangian and Hamiltonian Methods for Nonlinear Control 2006*, 61–73. Springer.

Cardoso-Ribeiro, F.L., Pommier-Budinger, V., Schotte, J.S., and Arzelier, D. (2014). Modeling of a coupled fluid-structure system excited by piezoelectric actuators. In *2014 IEEE/ASME International Conference on Advanced Intelligent Mechatronics*, 216–221. IEEE.

Duindam, V., Macchelli, A., Stramigioli, S., and Bruyninckx, H. (2009). *Modeling and control of complex physical systems*. Springer.

Golo, G., Talasila, V., van der Schaft, A., and Maschke, B. (2004). Hamiltonian discretization of boundary control systems. *Automatica*, 40(5), 757–771.

Hamroun, B. (2009). *Approche hamiltonienne à ports pour la modélisation, la réduction et la commande des systèmes non linéaires à paramètres distribués: application aux écoulements*. Ph.D. thesis, Grenoble INP.

Hamroun, B., Dimofte, A., Lefèvre, L., and Mendes, E. (2010). Control by Interconnection and Energy-Shaping Methods of Port Hamiltonian Models. Application to the Shallow Water Equations. *European Journal of Control*, 16(5), 545–563.

Hodges, D.H. and Pierce, G.A. (2011). *Introduction to Structural Dynamics and Aeroelasticity*. Cambridge University Press.

Kunkel, P. and Mehrmann, V.L. (2006). *Differential-algebraic Equations: Analysis and Numerical Solution*. European Mathematical Society.

Matignon, D. and Hélie, T. (2013). A class of damping models preserving eigenspaces for linear conservative port-Hamiltonian systems. *European Journal of Control*, 19(6), 486–494.

Moulla, R., Lefévre, L., and Maschke, B. (2012). Pseudo-spectral methods for the spatial symplectic reduction of open systems of conservation laws. *Journal of Computational Physics*, 231(4), 1272–1292.

Petit, N. and Rouchon, P. (2002). Dynamics and solutions to some control problems for water-tank systems. *IEEE Transactions on Automatic Control*, 47(4), 594–609.

van der Schaft, A. and Maschke, B. (1994). On the Hamiltonian formulation of nonholonomic mechanical systems. *Rep. Math. Phys.*, 34(2), 225–233.

Voss, T. and Scherpen, J. (2014). Port-Hamiltonian Modeling of a Nonlinear Timoshenko Beam with Piezo Actuation. *SIAM Journal on Control and Optimization*, 52(1), 493–519.

Wu, Y., Hamroun, B., Le Gorrec, Y., and Maschke, B. (2014). Port Hamiltonian System in Descriptor Form for Balanced Reduction : Application to a Nanotweezer. In *The 19th World Congress of the International Federation of Automatic Control*. Cape Town, South Africa.

Appendix A. DISCRETIZATION

For all cases, the finite-dimensional approximation obtained through mixed finite-element methods leads to an equation like:

$$\frac{\partial}{\partial t}\begin{bmatrix}\boldsymbol{x_1}\\ \boldsymbol{x_2}\end{bmatrix} = \begin{bmatrix}0 & M\\ -M^T & 0\end{bmatrix}\begin{bmatrix}\partial_{x_1}H\\ \partial_{x_2}H\end{bmatrix} + \begin{bmatrix}0 & B_1\\ B_2 & 0\end{bmatrix}u, \qquad (A.1)$$

$$y = \begin{bmatrix}0 & B_2^T\\ B_1^T & 0\end{bmatrix}\begin{bmatrix}\partial_{x_1}H\\ \partial_{x_2}H\end{bmatrix} + \begin{bmatrix}0 & D\\ -D^T & 0\end{bmatrix}u. \qquad (A.2)$$

The values of matrices M, B_1, B_2 and D, as well as the dimensions of u and y depends on the differential operator $\mathcal{J}$. Torsion and Saint-Venant equations have both a first-order $\mathcal{J}$, whereas Euler-Bernoulli has a second-order one.

A.1 Torsion and Saint-Venant equation

In this case, $u = [e_1(L)\ e_2(0)]^T$, $y = [-e_2(L)\ e_1(0)]^T$. The matrices M, B_1, B_2 and D are not shown here since they can be obtained from Hamroun (2009) (Section 2.2.3).

Discretization of torsion Hamiltonian. From Eq. 11:

$$H^T(x_1^T, x_2^T) = \sum_{i=1}^{N}\frac{1}{2}\int_{z=(i-1)\Delta z}^{i\Delta z}\left(GJ(x_1^T)^2 + \frac{(x_2^T)^2}{I_p}\right)dz, \qquad (A.3)$$

where $\Delta z = L/N$ is the length of each element. Assuming constant material coefficients and $x_1^T(z_i,t) = x_{1,i}^T(t)/\Delta z$, inside each element:

$$H_d^T(x_{1,i}^T, x_{2,i}^T) = \sum_{i=1}^{N}\frac{1}{2\Delta z}\left(GJ(x_{1,i}^T)^2 + \frac{(x_{2,i}^T)^2}{I_p}\right), \quad (A.4)$$

This easily allows us to calculate the co-energy variables:

$$e_{1,i}^T = \frac{\partial H_d}{\partial x_{1,i}^T} = \frac{GJ}{\Delta z}x_{1,i}^T, \qquad (A.5)$$

$$e_{2,i}^T = \frac{\partial H_d}{\partial x_{2,i}^T} = \frac{1}{I_p\Delta z}x_{2,i}^T. \qquad (A.6)$$

Discretization of Saint-Venant Hamiltonian

$$H^F(\alpha_1,\alpha_2,\theta,p_f) = \sum_{i=1}^{N}\int_{z_{i-1}}^{z_i}\left(\rho g\bar{h}^2\frac{\alpha_1^2}{2} + \frac{\alpha_2^2}{2\rho\bar{h}b} \right. \qquad (A.7)$$
$$\left. + \rho g z\bar{h}\alpha_1\theta\right)dz + \frac{p_f^2}{2I_f},$$

$$H_d^F(\alpha_{1,i},\alpha_{2,i},\theta,p_f) = \sum_{i=1}^{N}\left(\frac{\rho g\bar{h}^2\alpha_{1,i}^2}{2\Delta z} + \frac{\alpha_{2,i}^2}{2\rho b\bar{h}\Delta z} + \right. \qquad (A.8)$$
$$\left. + \frac{\rho g\bar{h}\alpha_{1,i}\theta(z_i^2 - z_{i-1}^2)}{2\Delta z}\right) + \frac{p_f^2}{2I_f}.$$

$$e_{1,i}^F = \frac{\partial H_d}{\partial \alpha_{1,i}^T} = \frac{\rho g\bar{h}^2}{\Delta z}\alpha_{1,i}^F + \frac{\rho g\bar{h}\theta(z_i^2 - z_{i-1}^2)}{2\Delta z}, \qquad (A.9)$$

$$e_{2,i}^F = \frac{\partial H_d}{\partial \alpha_{2,i}^T} = \frac{1}{\rho b\bar{h}\Delta z}\alpha_{2,i}^F, \qquad (A.10)$$

$$e_\theta^F = \frac{\partial H_d}{\partial \theta} = \sum_{i=1}^{N}\frac{\rho g\bar{h}\alpha_{1,i}(z_i^2 - z_{i-1}^2)}{2\Delta z}, \qquad (A.11)$$

$$e_{p_f}^F = \frac{\partial H_d}{\partial p_f} = \frac{p_f}{I_f} = \dot{\theta}. \qquad (A.12)$$

A.2 Euler-Bernoulli equation

In this case, $\boldsymbol{u} = \left[e_0^2\ e_0^{2\partial}\ e_L^1\ e_L^{1\partial}\right]^T$ and output $\boldsymbol{y} = \left[-e_0^{1\partial}\ e_0^1\ -e_L^{2\partial}\ e_L^2\right]^T$. Using a similar development from Bassi et al. (2007), we've found the following matrices:

$$M = \begin{bmatrix}m_1 & 0 & \dots & 0\\ m_2 & m_1 & \dots & 0\\ \vdots & \vdots & \ddots & \vdots\\ m_N & m_{N-1} & \dots & m_1\end{bmatrix}, \qquad (A.13)$$

where:

$$m_1 = -\frac{\bar{\alpha}}{\alpha^2}, \qquad (A.14)$$

$$m_i = \bar{\alpha}\frac{(2\alpha - i)(\alpha-1)^{i-3}}{\alpha^{i+1}}, \quad i = 2,3,\dots,N, \qquad (A.15)$$

with $\bar{\alpha} = 1/\Delta z$ and $\alpha = 0.5$, when using spline approximation.

$$D = \begin{bmatrix}-N\bar{\alpha}\frac{(\alpha-1)^{N-1}}{\alpha^{N+1}} & -\left(\frac{\alpha-1}{\alpha}\right)^N\\ \left(\frac{\alpha-1}{\alpha}\right)^N & 0\end{bmatrix}, \qquad (A.16)$$

$$B_{12} = \begin{bmatrix}b_{11} & b_{12}\\ b_{21} & b_{22}\\ \vdots & \vdots\\ b_{N1} & b_{N2}\end{bmatrix}, \quad B_{34} = \begin{bmatrix}-b_{N1} & b_{N2}\\ -b_{(N-1)1} & b_{(N-1)2}\\ \vdots & \vdots\\ -b_{11} & b_{12}\end{bmatrix}, \qquad (A.17)$$

where:

$$b_{i1} = \bar{\alpha}\frac{(\alpha - i)(\alpha-1)^{i-2}}{\alpha^{i+1}}, \quad i = 1,2,3,\dots,N, \qquad (A.18)$$

$$b_{i2} = \frac{(\alpha-1)^{i-1}}{\alpha^i}, \quad i = 1,2,3,\dots,N. \qquad (A.19)$$

Discretization of Euler-Bernoulli Hamiltonian

$$H^B(x_1^B, x_2^B) = \frac{1}{2}\sum_{i=1}^{N}\int_{(i-1)\Delta z}^{i\Delta z}\left(\frac{1}{\mu}(x_1^B)^2 + EI(x_2^B)^2\right)dz, \qquad (A.20)$$

$$H_d^B(x_{1,i}^B, x_{2,i}^B) = \frac{1}{2}\sum_{i=1}^{N}\left(\frac{1}{\mu\Delta z}(x_{1,i}^B)^2 + \frac{EI}{\Delta z}(x_{2,i}^B)^2\right), \qquad (A.21)$$

$$e_{1,i}^B = \frac{\partial H_d^B}{\partial x_{1,i}^B} = \frac{1}{\mu\Delta z}x_{1,i}^B, \qquad (A.22)$$

$$e_{2,i}^B = \frac{\partial H_d^B}{\partial x_{2,i}^B} = \frac{EI}{\Delta z}x_{2,i}^B. \qquad (A.23)$$